

This Accepted Author Manuscript is copyrighted and published by Elsevier. It is posted here by agreement between Elsevier and University of Brasilia. Changes resulting from the publishing process - such as editing, corrections, structural formatting, and other quality control mechanisms - may not be reflected in this version of the text. The definitive version of the text was subsequently published in [Theriogenology, Volume 76, Issue 9, December 2011, Pages 1647–1657, doi:10.1016/j.theriogenology.2011.06.029]. You may download, copy and otherwise use the AAM for non-commercial purposes provided that your license is limited by the following restrictions:

- (1) You may use this AAM for non-commercial purposes only under the terms of the CC-BY-NC-ND license.
- (2) The integrity of the work and identification of the author, copyright owner, and publisher must be preserved in any copy.
- (3) You must attribute this AAM in the following format: [agreed attribution language, including link to CC BY-NC-ND license + Digital Object Identifier link to the published journal article on Elsevier's ScienceDirect® platform].

---

Este Manuscrito do Autor Aceito para Publicação (AAM) é protegido por direitos autorais e publicado pela Elsevier. Ele está disponível neste Repositório, por acordo entre a Elsevier e a Universidade de Brasília. As alterações decorrentes do processo de publicação - como a edição, correção, formatação estrutural, e outros mecanismos de controle de qualidade - não estão refletidas nesta versão do texto. A versão definitiva do texto foi posteriormente publicado em [Theriogenology, Volume 76, Número 9, Dezembro 2011, Pages 1647–1657, doi:10.1016/j.theriogenology.2011.06.029]. Você pode baixar, copiar e utilizar de outra forma o AAM para fins não comerciais, desde que sua licença seja limitada pelas seguintes restrições:

- (1) Você pode usar este AAM para fins não comerciais apenas sob os termos da licença CC- BY-NC-ND.
- (2) A integridade do trabalho e identificação do autor, detentor dos direitos autorais e editor deve ser preservado em qualquer cópia.
- (3) Tem de atribuir este AAM no seguinte formato: [acordo na linguagem atribuída, incluindo o link para CC BY-NC-ND licença Digital + DOI do artigo publicado na revista Elsevier ScienceDirect® da plataforma].

# Ultrastructural characterization of porcine oocytes and adjacent follicular cells during follicle development: Lipid component evolution

Renata C. Silva  
Sônia N. Bão  
José Luiz P.R. Jivago  
Carolina M. Lucci

## Abstract

The objective of this study was to characterize the morphometry and ultrastructure of porcine preantral and antral follicles, especially the lipid component evolution. Ovarian tissue was processed for light microscopy. Ovarian tissue and dissected antral follicles (< 2, 2–4, and 4–6 mm) were also processed for transmission electron microscopy using routine methods and using an osmium-imidazole method for lipid detection. Primordial follicles ( $34 \pm 5 \mu\text{m}$  in diameter, mean  $\pm$  SD) had one layer of flattened-cuboidal granulosa cells around the oocyte, primary follicles ( $40 \pm 7 \mu\text{m}$ ) had a single layer of cuboidal granulosa cells around the oocyte, and secondary follicles ( $102 \pm 58 \mu\text{m}$ ) had two or more layers of cuboidal granulosa cells around the oocyte. Preantral follicle oocytes had many round mitochondria and both rough and smooth endoplasmic reticulum. In oocytes of primordial and primary follicles, lipid droplets were abundant and were mostly located at the cell poles. In secondary and antral follicles, the zona pellucida completely surrounded the oocyte, whereas some microvilli and granulosa cells projected through it. Numerous electron-lucent vesicles and vacuoles were present in the oolemma of secondary and antral follicles. Based on osmium-imidazole staining, most of these structures were shown to be lipid droplets. As the follicle developed, the appearance of the lipid droplets changed from small and black to large and gray, dark or dark with light streaks, suggesting that their nature may change over time. In summary, although porcine follicles and oocytes had many similarities to those of other mammalian species, they were rich in lipids, with lipid droplets with varying morphological patterns as the follicle developed.

**Keywords:** Preantral ovarian follicle; Lipids; Oocyte; Pig; Electron microscopy

## 1. Introduction

The mammalian ovary contains a large number of oocytes within ovarian follicles. Ovarian follicles comprise oocytes surrounded by supporting cells and can be classified as preantral (primordial, primary, and secondary) and antral (tertiary and Graafian) follicles. During folliculogenesis, numerous morphological and functional changes occur in the oocyte [1] and [2]. Knowledge of ovarian follicle and oocyte morphology is crucial to the development of assisted reproductive techniques, such as oocyte cryopreservation and in vitro embryo production.

Morphometric and ultrastructural studies of follicles and oocytes have been described for cattle [1] and [3], sheep [4], goats [5] and [6], buffalo [7] and [8], cats [9], and humans [10]

and [11]. These studies demonstrated differences among species. In pigs, Greewald and Moor [12] described the morphology and ultrastructure of isolated primordial follicles. The ultrastructure of follicular porcine granulosa cells have also been reported [13] in a study of the steroidogenic process performed by these cells. However, morphometric and ultrastructural characterizations of porcine follicles at all their developmental stages have not yet been completely described. Moreover, many reports are now using ultrastructural studies as tools to evaluate the damage or changes caused by assisted reproductive techniques, especially cryopreservation of fully grown oocytes [14], [15], [16] and [17]. Porcine oocytes typically contain large amounts of cytoplasmic lipids that are major obstacles to efficient cryopreservation [18]. Conversely, preantral follicles have been cited as an alternative strategy for storing female germ cells in pigs [19] and other species. Oocytes within preantral follicles have several characteristics that may make them less vulnerable to cryoinjury than fully grown oocytes, including a reduced amount of lipids [20]. These statements emphasized the need to have a single comprehensive study describing in detail the features of oocytes and follicular cells at all developmental stages.

The aim of the present work was to describe the ultrastructure of porcine oocytes and adjacent cells from preantral and antral ovarian follicles, especially changes in the lipid component of these cells.

## **2. Materials and methods**

### **2.1. Ovary collection**

Ovaries from prepubertal gilts (crossbreeding females) were collected at a local abattoir and transported to the laboratory in saline solution (0.9% NaCl) at 37 °C within 1 h after collection. In the laboratory, ovaries were trimmed and rinsed with 70% ethanol and sterile saline. Cortex samples were taken for evaluation of preantral follicles (primordial, primary, and secondary). Antral follicles were dissected under a stereomicroscope and divided into three groups: <2, 2–4, and 4–6 mm.

### **2.2. Light microscopy evaluation**

Only preantral follicles were analyzed by light microscopy. Pieces (~ 1 cm<sup>2</sup>) of ovarian cortex were fixed in Carnoy's fixative for 4 h, dehydrated in ethanol, clarified with xylene, and

embedded in paraffin wax. Semi-serial sections (5  $\mu\text{m}$ ) were stained with hematoxylin and eosin (HE) and examined with a Zeiss Axiophot brightfield light microscope (Zeiss, Oberkochen, Germany).

Preantral follicles were classified according to their developmental stage: primordial (one layer of flattened or flattened-cuboidal granulosa cells around the oocyte), primary (one layer of cuboidal granulosa cells around the oocyte), or secondary (two or more layers of cuboidal granulosa cells around the oocyte). Only morphologically normal follicles (MNF) with a visible nucleus were evaluated. Images were captured with a digital CCD camera (Sony DXC-107A, Tokyo, Japan), and measurements were performed with the aid of morphometric analysis software (Image Pro-Plus 5.1, MediaCybernetics, Bethesda, MD, USA). Granulosa cell counts and diameter measurements of follicles, oocytes, and oocyte nuclei were always obtained from the equatorial section of primordial (N = 113), primary (N = 76), and secondary (N = 27) follicles.

### **2.3. Transmission electron microscopy**

All electron microscopy reagents were purchased from Electron Microscopy Sciences (Hatfield, PA, USA).

Primordial (N = 10), primary (N = 9), secondary (N = 6), and antral follicles (N = 14) were evaluated by transmission electron microscopy. Sample preparation included both routine preparation and the osmium-imidazole method (lipid detection). Portions of ovarian cortex ( $\sim 1 \text{ mm}^2$ ) and dissected antral follicles were fixed in Karnovsky's fixative (2% paraformaldehyde, 2.5% glutaraldehyde in 0.1 M sodium cacodylate buffer, pH 7.2) for 4 h at room temperature. Samples were postfixed in solution containing 1% osmium tetroxide, 0.8% potassium ferricyanide, and 5 mM calcium chloride and contrasted en bloc with uranyl acetate. Samples were then dehydrated in acetone and embedded in Spurr.

Lipid detection was performed using the osmium-imidazole method. Following routine fixation (as described above), ovarian cortical samples and follicles from each antral group were washed with sodium cacodylate buffer (0.1 M) and then in imidazole buffer (0.1 M) before being postfixed in a solution containing 2% osmium tetroxide in 0.1 M imidazole buffer (30 min). Samples were then washed in imidazole buffer, dehydrated in acetone, and embedded in Spurr.

Semi-thin sections (3  $\mu\text{m}$ ) were stained with toluidine blue and examined under a light microscope to localize oocytes in normal follicles. Ultra-thin sections (70 nm) were examined using a Jeol 1011 transmission electron microscope (Jeol, Tokyo, Japan). The characteristics of oocyte and granulosa cell cytoplasm, the presence and distribution of organelles, and the

appearance of nuclear and plasma membranes and the zona pellucida were observed and recorded.

## 2.4. Statistical analysis

Follicle, oocyte and oocyte nucleus diameters, and granulosa cell numbers were compared among follicular classes. Data were analyzed by ANOVA and Scheffè's test (StatView for Windows, SAS Institute Inc., Cary, NC, USA).

## 3. Results

### 3.1. Light microscopy

Primordial follicles contained an oocyte surrounded by a single layer of flattened granulosa cells (Fig. 1A). Cuboidal granulosa cells were present in some primordial follicles, usually at only one pole of the follicle. Primary follicles had one layer of cuboidal granulosa cells around the oocyte (Fig. 1B). Follicles with two or more layers of cuboidal granulosa cells were classified as secondary follicles (Fig. 1C and D). Early secondary follicles still lacked a well-developed zona pellucida (Fig. 1C). Oocytes from late secondary and antral follicles were completely surrounded by a zona pellucida (Fig. 1D and E). All preantral follicles were delimited from the stroma by a basement membrane. Follicle, oocyte and oocyte nucleus diameters and the number of granulosa cells in primordial, primary, and secondary follicles are presented in Table 1.

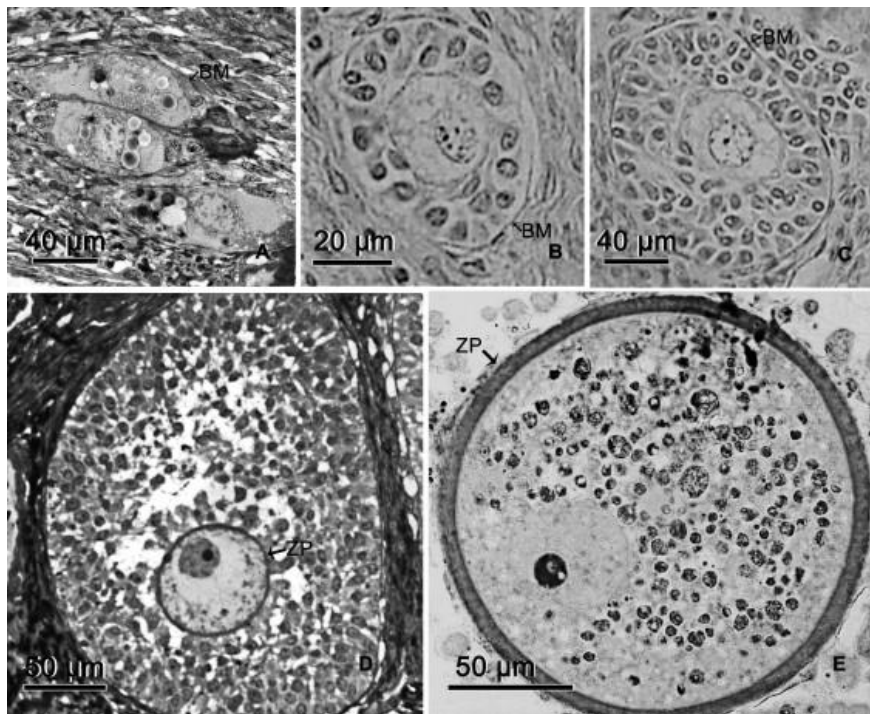


Fig. 1. Semi-thin section of porcine ovaries with: (A) primordial follicles; (B) primary follicle; (C) early and (D) late secondary follicles; and (E) tertiary follicle oocyte. ZP, zona pellucida; BM, basement membrane.

Table 1.

Diameters of follicles, oocytes and oocyte nuclei ( $\mu\text{m}$ ) and granulosa cell number in porcine preantral ovarian follicles. Mean  $\pm$  SD and range are given.

Follicle class	No.	Follicle diameter ( $\mu\text{m}$ )	Oocyte diameter ( $\mu\text{m}$ )	Nucleus diameter ( $\mu\text{m}$ )	No. granulosa cells
Primordial	113	33.8 $\pm$ 3.4 <sup>a</sup> (23–52)	26.0 $\pm$ 2.5 <sup>a</sup> (18–36)	14.7 $\pm$ 1.6 <sup>a</sup> (8–20)	5.2 $\pm$ 2.4 <sup>a</sup> (1–17)
Primary	76	40.4 $\pm$ 5.1 <sup>b</sup> (23–67)	27.3 $\pm$ 2.8 <sup>b</sup> (20–38)	15.2 $\pm$ 1.7 <sup>a</sup> (9–22)	8.4 $\pm$ 3.9 <sup>b</sup> (1–22)
Secondary	27	84.5 $\pm$ 15.1 <sup>c</sup> (36–142)	39.1 $\pm$ 6.8 <sup>c</sup> (22–66)	19.6 $\pm$ 3.6 <sup>b</sup> (11–34)	49.7 $\pm$ 22.8 <sup>c</sup> (30–90)

a-c Within a column, means without a common superscript differed ( $P < 0.05$ ).

## 3.2. Ultrastructure

### 3.2.1. Primordial follicles

Primordial follicles had an oval or spherical oocyte with a large homogeneous cytoplasm. An oval, centrally located nucleus had loose chromatin and occasionally displayed a nucleolus. Organelles were distributed throughout the ooplasm (Fig. 2A). The most abundant organelles were round mitochondria with peripheral cristae, and electron-dense granules and vacuoles were usually observed in the mitochondrial matrix (Fig. 2B). There was substantial endoplasmic reticulum, either associated with mitochondria or free in the oocyte cytoplasm (Fig. 2B). Small vesicles were consistently present, but Golgi cisternae were rare. Lipid droplets appeared as small dark round structures and were always present in abundance (Fig. 2A and B). Lipid droplets were sometimes surrounded by smooth endoplasmic reticulum (Fig. 2B). Polyribosomes were observed on the surface of rough endoplasmic reticulum or free throughout the oolemma (Fig. 2C). The cellular membranes of the oocyte and adjacent granulosa cells were juxtaposed, and coated pits were occasionally observed in the oocyte outer cortex. Zones of adhesion and some microvilli were also observed (Fig. 2D). Granulosa cells were flattened and their nuclei were irregular and elongated, containing mainly loose chromatin and some patches of condensed chromatin (Fig. 2A and D). In these cells, endoplasmic reticulum and mitochondria were the predominant organelles, and lipid droplets were present.

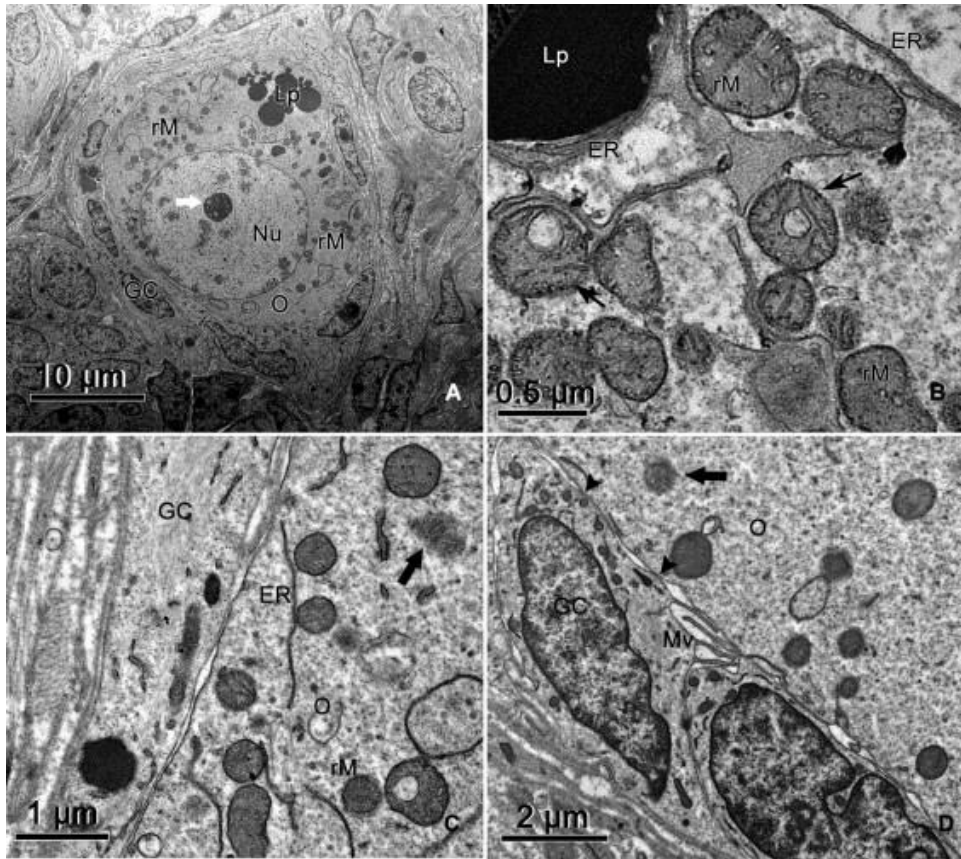
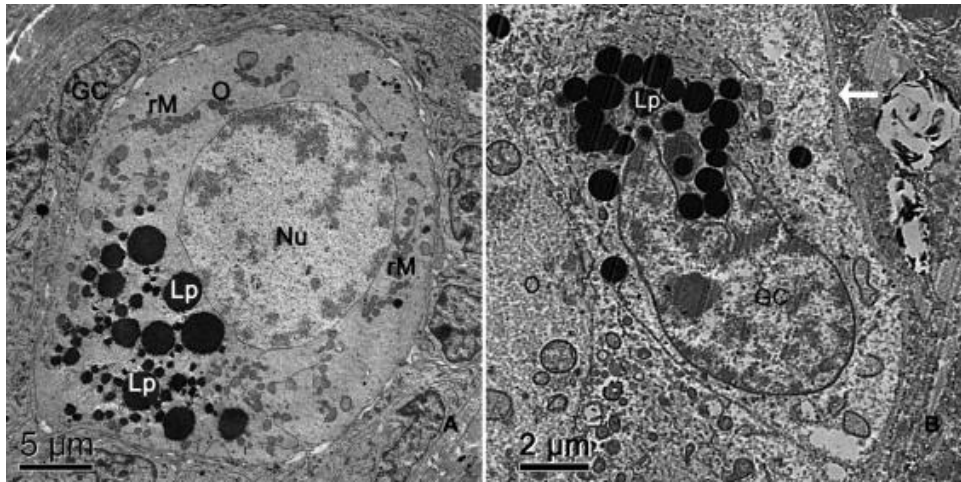


Fig. 2. Electron micrographs of porcine primordial ovarian follicles. (A) Overview and (B) detail of round mitochondria presenting vacuoles (thin arrows) in the matrix. Note the association among lipid droplets, mitochondria and smooth endoplasmic reticulum. (C) Free polyribosomes (thick arrow) were often observed throughout the oolemma. (D) At the primordial stage, oocyte and granulosa cell membranes are juxtaposed, and zones of adhesion (arrowheads) and microvilli were observed. Nu, oocyte nucleus; O, oocyte; GC, granulosa cell; Lp, lipid droplet; rM, round mitochondria; ER, endoplasmic reticulum; Mv, microvilli. The thick white arrow indicates the nucleolus.

### 3.2.2. Primary follicles

The oocytes of primary follicles were spherical or oval, with a central and spherical nucleus. Organelles were still distributed throughout the ooplasm (Fig. 3A). Lipid droplets and round mitochondria were abundant, and mitochondria were usually associated with smooth endoplasmic reticulum (Fig. 3A). Golgi cisternae were rare. Granulosa cells were cuboidal; their cytoplasmic ultrastructure was similar to that of primordial follicles but showed more abundant lipid droplets (Fig. 3B). Oocyte and granulosa cell membranes were still juxtaposed, and occasionally the oolemma seemed to invade spaces between two adjacent granulosa cells.



### 3.2.3. Secondary follicles

In secondary follicle oocytes, the organelles were located at the periphery of the cell (Fig. 4A) as was the nucleus (Fig. 1D). Round mitochondria were organized as strings of pearls (Fig. 4B) and were the most abundant organelles. Elongated mitochondria remained rare (Fig. 4C). Golgi apparatus (Fig. 4D) and endoplasmic reticulum cisternae (Fig. 4E) were dilated. Dark lipid droplets were no longer present, and the oocyte cytoplasm was instead full of electron-lucent vesicles (Fig. 4A). The zona pellucida began to form in secondary follicles. Although early secondary follicles did not yet display a well-developed zona pellucida (Fig. 4A), the zona pellucida was completely formed and surrounded the oocyte in late secondary follicles (Fig. 4E and F); some microvilli and granulosa cell projections ending in gap junctions penetrated it (Fig. 4F). All granulosa cells were cuboidal, with organelles that seemed to be more developed in comparison to primordial and primary follicle granulosa cells. Round mitochondria and endoplasmic reticulum were the most abundant organelles.

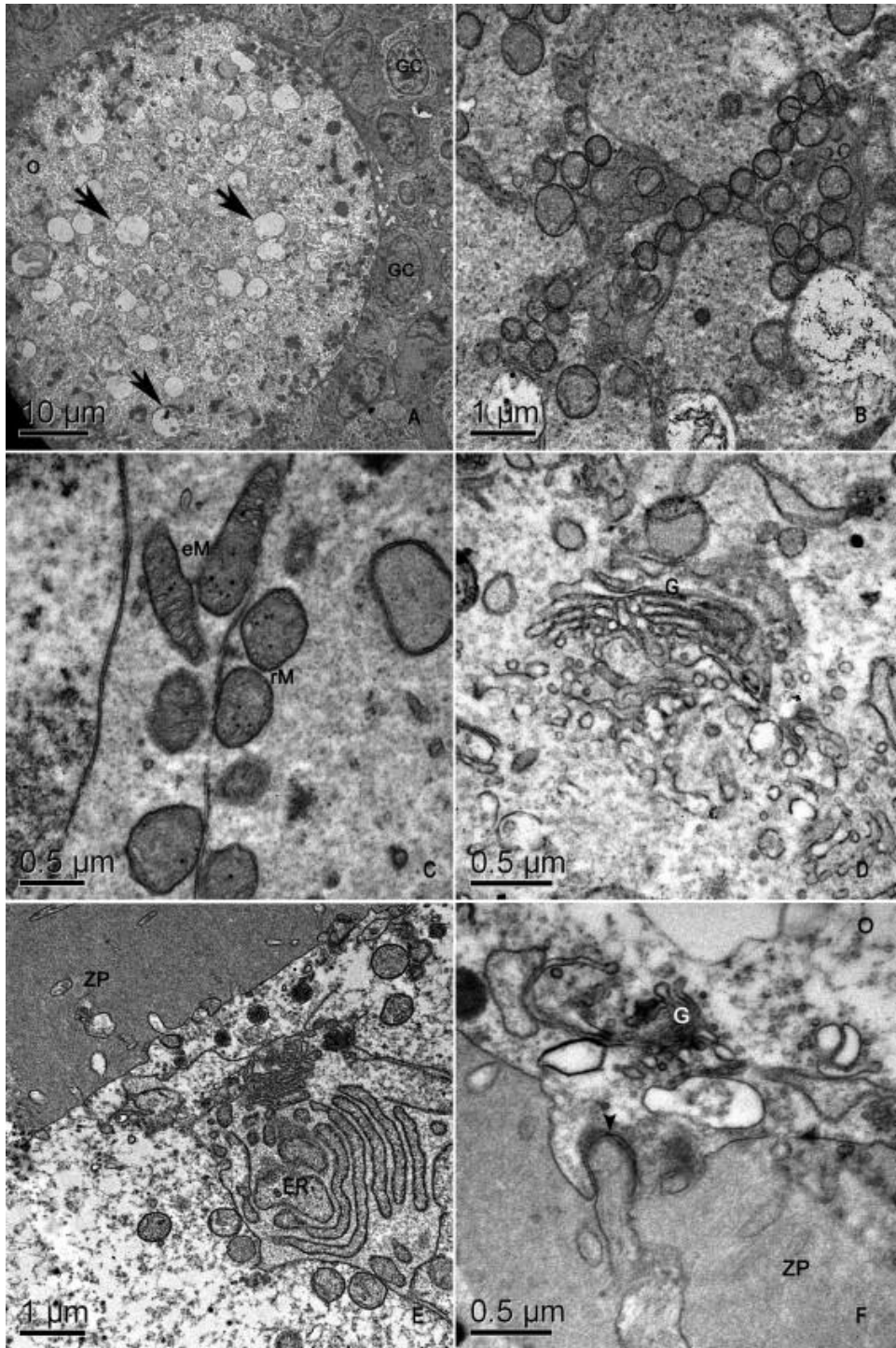


Fig. 4. Electron micrographs of pig secondary follicles. (A) An overview. Note the presence of many vesicles in the oolemma (arrows). (B) Mitochondria organized as strings of pearls. (C) Details of mitochondria. (D) Golgi apparatus. (E) Detail of endoplasmic reticulum. (F) Detail of granulosa cell projection through the zona pellucida ending in gap junction (arrowhead). O, oocyte; GC, granulosa cell; rM, round mitochondria; eM, elongated mitochondria; G, Golgi apparatus; ER, endoplasmic reticulum; ZP, zona pellucida.

### 3.2.4. Tertiary follicles

In general, the three groups of antral follicles (< 2, 2–4, and 4–6 mm) had similar ultrastructures. They contained a spherical oocyte with a circular nucleus located at the oocyte periphery (Fig. 5A). Again, round mitochondria were abundant (Fig. 5B), but many elongated and some pleomorphic mitochondria were also observed. The Golgi complex appeared to have increased in size but with less-dilated cisternae. The free form of smooth and rough endoplasmic reticulum became less extensive. The oocyte cytoplasm was full of electron-lucent structures (Fig. 5A). These structures were often in close proximity to mitochondria and smooth endoplasmic reticulum. All oocytes were surrounded by a zona pellucida. Granulosa cell projections through the zona pellucida (Fig. 5C) ended in indentations on the oolemma. Additionally, erect and bent microvilli from the oocyte penetrated the zona pellucida (Fig. 5C). The development of perivitelline space was associated with the liberation of microvilli from the zona pellucida and was more evident when follicles were > 2 mm. Coated pits were nearly absent in oocytes of 2-mm follicles and were absent in the other antral classes. Granulosa cells surrounding the oocyte, now termed cumulus cells, had small antral spaces among them (Fig. 5D). Mitochondria and rough endoplasmic reticulum were still the most abundant organelles in these cells.

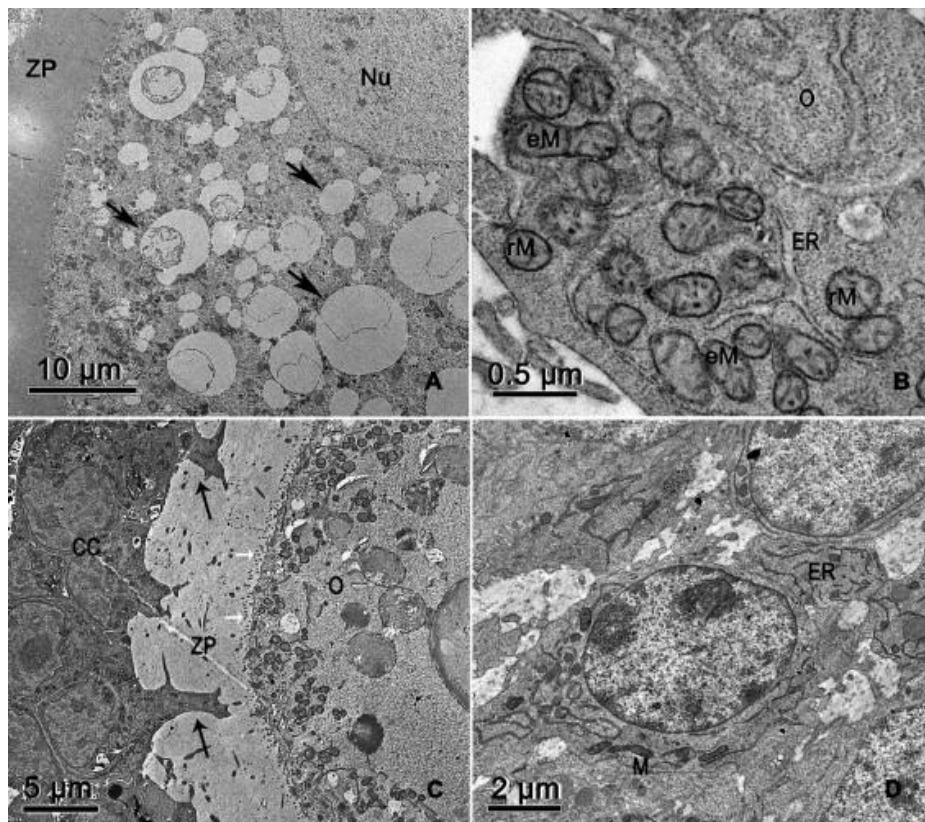


Fig. 5. Electron micrographs of antral follicle oocytes. (A) Oocyte with peripheral nucleus. Note the presence of many vacuoles in the oolemma (thick arrows). (B) Detail of mitochondria. (C) Detail of zona pellucida with granulosa cell projections (thin arrows) and oocyte microvilli (white arrows) running through it. (D) Detail of cumulus cells. Note the small antral spaces among them. Nu, oocyte nucleus; O, oocyte; eM, elongated mitochondria; rM, round mitochondria; ER, endoplasmic reticulum; ZP, zona pellucida; CC, cumulus cell.

### 3.2.5. Osmium-imidazole method

When the osmium-imidazole method was applied to primordial and primary follicles, there was no difference in the appearance of the lipid droplets, which appeared as small, dark, round structures. Interestingly, in secondary and tertiary follicles, large differences were noted before and after the osmium-imidazole procedure. In secondary follicles, some of the electron-lucent vesicles (Fig. 4A) appeared as dark structures (Fig. 6A), indicating that they were in fact lipid droplets, whereas others remained gray (Fig. 6B). In tertiary follicles, the large electron-lucent structures (Fig. 5A) were also lipid droplets. They had various sizes, shapes and electron densities (Fig. 6C). Some were dark with electron-lucent streaks (Fig. 6D).

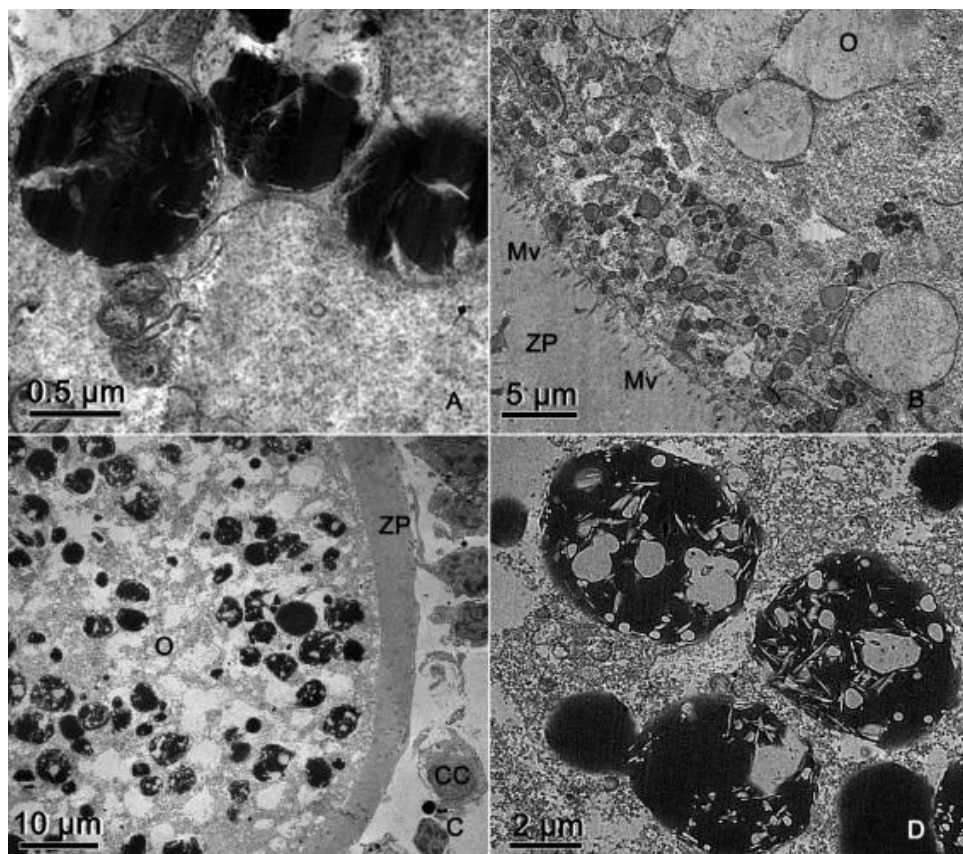


Fig. 6. Appearance of lipid droplets after osmium-imidazole staining in the oocyte cytoplasm of secondary (A and B) and antral follicles (C and D). Note the dark (A) or gray (B) lipid droplets in secondary follicle oocytes. In antral follicle oocytes lipid droplets displayed different sizes, shapes and electron densities (C), often appearing dark with electron-lucent streaks (D). O, oocyte; CC, cumulus cell; ZP, zona pellucida; Mv, microvilli.

## 4. Discussion

In this study, the diameters of preantral follicles and their oocytes were similar to those described for some other mammals, e.g., cattle [3] and marsupials [21], and were larger than those of goats [6], sheep [22], buffalos [8], and capuchin monkeys [23]. Some secondary follicles 250 to 351  $\mu\text{m}$  in diameter were observed (data not shown), confirming that antral formation occurred later in porcine follicles (400  $\mu\text{m}$ ) [24] than in bovine follicles (200  $\mu\text{m}$ ) [25]. The present work classified primordial follicles as an oocyte surrounded by flattened or flattened/cuboidal granulosa cells. Some authors classify these follicles as intermediary follicles [26].

In general, the ultrastructure of swine preantral follicles was similar to those of other mammalian species (human [27], goat [6], cow [3] and [28], and cat [9]). Antral follicles also displayed similarities to other species (cows [2], wild-type sheep [29], and buffalos [8]). However, some differences were observed.

Round mitochondria were the most abundant organelles in porcine oocyte cytoplasm in all follicle classes studied. This was also described for preantral follicles of other species, such as buffalos [8] and cows [3]. However, Lucci et al [6] described that elongated mitochondria predominated in goat secondary follicle oocytes. In this study, elongated and pleomorphic mitochondria were observed in tertiary follicles. Fair et al [2] suggested that round mitochondria may be an immature mitochondrial form from which all other forms arise. Several mitochondria presented electron-dense granules and vacuoles in their matrix. These granules were also described in bovine oocyte mitochondria [3]. According to Fawcett et al [30], these granules are present in ion-transporting tissues such as liver, kidney, and pancreas and are related to mitochondrial control of ions. Gunter and Gunter [31] described these granules as calcium deposits.

The present study detected a more-developed smooth and rough endoplasmic reticulum in secondary and tertiary follicles. In buffalo oocytes, Mondadori et al [7] and [8] described the same pattern. The smooth endoplasmic reticulum functions in several metabolic processes, including lipid and steroid synthesis, carbohydrate metabolism, and calcium concentration regulation [32]. Considering that primordial follicle oocytes are quiescent, smooth endoplasmic reticulum is more evident in growing follicle oocytes with intense metabolic activity, such as secondary and tertiary follicles. Similarly, rough endoplasmic reticulum is involved with protein synthesis, including the zona pellucida glycoproteins [33]. It is thus expected that rough endoplasmic reticulum would be more developed in oocytes from late secondary and tertiary follicles, which have a thick zona pellucida. An intense association between mitochondria and endoplasmic reticulum was also observed. Bernhard and Rouiller [34] affirmed that this association indicated a physiologic relationship, with mitochondria providing energy for the regrowth and activity of endoplasmic reticulum.

In this study, the zona pellucida completely surrounded the oocyte only in secondary follicles, as reported in cattle [2] and [35] and goats [6]. However, the zona pellucida was seen at the primary follicle stage in the guinea pig [36], monkey [37], rabbit [38], human [39], mouse [40], and cat [9].

Thicker zona pellucida corresponded to greater numbers of microvilli and granulosa cell projections. The large quantity of microvilli may represent a means of molecular transport between granulosa cells and the oocyte. We observed that granulosa cell projections ended in gap junctions. Evidence indicates that somatic cell-oocyte interactions via gap junctions are essential for oocyte growth and metabolism. This is one of the routes by which granulosa cells supply ions, nucleotides and amino acids to the oocyte [41] and [42]. According to Fair et al [2], in primordial and primary follicles, the numerous coated pits present in the cortical ooplasm compensate for the absence of specific communication channels. Granulosa cell-oocyte intercommunication may occur through receptor-mediated endocytosis during the initial period of oocyte growth, with subsequent redirection to cell-to-cell gap-junction coupling [41] when the zona pellucida is completely developed.

The biggest difference between porcine follicles and those of other mammals was the high content of intracellular lipid in swine oocytes. Lipids are also present in bovine [43] and ovine [44] oocytes, though to a lesser extent. Granulosa cells also had an unusually large amount of lipid, particularly in porcine primordial and primary follicles. In addition, there were distinct lipid characteristics in various follicle classes. Primordial and primary follicle oocytes had a cytoplasm full of dark and round lipid droplets. In secondary and tertiary follicle oocytes, however, numerous electron-lucent structures were found, which were shown to be lipid droplets (based on osmium-imidazole staining). The presence of bright vesicles in the oocyte cytoplasm has been frequently reported [3], [6] and [8]. We concluded that, in the absence of a specific stain, some lipid droplets look like vesicles, and in many previous instances, may have been misclassified.

It was also observed that, in primordial and primary follicles, lipid droplets retained the same appearance using either osmium or osmium-imidazole staining. Imidazole is a weak organic base, which is soluble in water, alcohol, and lipids [45]. It stains highly saturated fatty acids, can also increase staining of unsaturated lipids and is the most effective method for staining phospholipids and lipoproteins [45]. Therefore, the morphological changes observed in lipid droplets during follicle development may reflect changes in the nature of the lipids being stored in those droplets. This is an interesting finding, as the quantity, nature, and distribution of lipids have important implications for the potential for oocyte and embryo cryopreservation, as lipids are sensitive to low temperatures, especially below 15 °C [15] and [46]. In that regard, the large amount of lipid in porcine oocytes has been implicated in the limited success with cryopreservation [18] and [47]. Moreover, abnormal changes in lipid droplets caused by cryopreservation have been reported [14], [15], [16] and [17] and seem to correspond with poor development.

After osmium-imidazole staining, lipid droplets from secondary follicle oocytes appeared as round, dark or gray structures, whereas lipid droplets from tertiary follicle oocytes appeared as dark structures with electron-lucent streaks. Isachenko et al [48] described two types of lipid droplets in porcine oocytes—dark homogeneous vesicles and gray vesicles with electron-lucent streaks. The authors suggested that this was a consequence of cytoplasmic lipolysis and that dark vesicles change to gray ones after lipid utilization.

In conclusion, morphometry of porcine preantral follicles was characterized, in association with the ultrastructure of porcine oocytes and adjacent follicular cells. Many changes that occurred in the oocyte during follicular development were documented. Notably, lipids were abundant in porcine oocytes at all stages of ovarian follicular development. In addition, changes in the appearance of lipid droplets as follicles develop suggest changes in the nature of the lipids. Morphological knowledge regarding porcine oocytes may be useful for development of various reproductive technologies. Furthermore, future studies of fatty acid composition in porcine ovarian follicles may be of interest.

#### Acknowledgments

The authors are grateful for financial support from FINEP, FAP-DF, CAPES, and CNPq.

#### References

- [1] Hyttel P, Xu KP, Smith S, Greve T. Ultrastructure of in-vitro oocyte maturation in cattle. *J Reprod Fert* 1986;78:615–25
- [2] Fair T, Hulshof SCJ, Hyttel P, Boland TM. Oocyte ultrastructure in bovine primordial to early tertiary follicles. *Anat Embryol* 1997;195:327–36.
- [3] Kacinskis MA, Lucci CM, Luque MCA, Báo SN. Morphometric and ultrastructural characterization of *Bos indicus* preantral follicles. *Anim Reprod Sci* 2005;47:45–57.
- [4] Hay MF, Cran DG, Moor RM. Structural changes occurring during atresia in sheep ovarian follicles. *Cell Tiss Res* 1976; 169:515–29.
- [5] Sharma RK, Sawhney AK. Fine morphology of membrane granulosa in caprine ovary. *Ind J Anim Sci* 1999;69:109–13.
- [6] Lucci CM, Silva RV, Carvalho CA, Figueiredo JR, Báo SN. Light microscopical and ultrastructural characterization of goat preantral follicles. *Small Rumin Res* 2001;41:61–9.
- [7] Mondadori RG, Santin TR, Fidelis AAG, Porfírio EP, Báo SN. Buffalo (*Bubalus bubalis*) preantral follicle population and ultrastructural characterization of antral follicle oocyte. *Reprod Dom Anim* 2010;45:33–7.
- [8] Mondadori RG, Luque MCA, Santin TR, Báo SN. Ultrastructural and morphometric characterization of buffalo (*Bubalus bubalis*) ovarian preantral follicles. *Anim Reprod Sci* 2007;97:323–33.
- [9] Carrijo-Junior OA, Marinho, APS, Campos AA, Amorim CA, Báo SN, Lucci CM. Morphometry, estimation and ultrastructure of ovarian preantral follicle population in queens. *Cell Tiss Org* 2010;191:152–60.
- [10] Bruin JP, Dorland SPEK, Posthuma MER, Van Haaften G, Looman M, TeVelde ER. Ultrastructure of the resting ovarian follicle pool in healthy young women. *Biol Reprod* 2002;66: 1151–60.
- [11] Westergaard CG, Byskov AG, Andersen CY. Morphometric characteristics of the primordial to primary follicle transition in the human ovary in relation to age. *Hum Reprod* 2007;22:2225–31.

- [12] Greenwald GS, Moor RM. Isolation and preliminary characterization of pig primordial follicles. *J Reprod Fert* 1989;87:561–71.
- [13] Bjersing L. On the ultrastructure of follicles and isolated follicular granulosa cells of porcine ovary. *Z Zellforsch Mikrosk Anat* 1967;82:173–86.
- [14] Wu C, Rui R, Dai J, Zhang C, Ju S, Xie B, Lu X, Zheng X. Effects of cryopreservation on the developmental competence, ultrastructure and cytoskeletal structure of porcine oocytes. *Mol Reprod Develop* 2006;73:1454–62.
- [15] Gerelchimeg B, Li-Qing L, Zhong Z, Jiang-Tian T, Qing-Ran K, Jun S, Xue-Dong W, Zhong-Hua L. Effect of chilling on porcine germinal vesicle stage oocytes at the subcellular level. *Cryobiology* 2009;59:54–8.
- [16] Fu X-W, Shi W-Q, Zhang Q-J, Zhao X-M, Yan CL, Hou Y-P, Zhou G-B, Fan Z-Q, Suo L, Wusiman A, Wang Y-P, Zhu S-E. Positive effects of Taxol pretreatment on morphology, distribution and ultrastructure of mitochondria and lipid droplets in vitrification of in vitro matured porcine oocytes. *Anim Reprod Sci* 2009;115:158–68.
- [17] Hao Z-D, Liu S, Wu Y, Wan P-C, Cui M-S, Chen H, Zeng S-M. Abnormal changes in mitochondria, lipid droplets, ATP and glutathione content, and Ca<sup>2+</sup> release after electro-activation contribute to poor developmental competence of porcine oocyte during in vitro ageing. *Reprod Fertil Develop* 2009;21:323–32.
- [18] Zhou G-B, Li N. Cryopreservation of porcine oocytes: recent advances. *Mol Hum Reprod* 2009;15:279–85.
- [19] Borges EN, Silva RC, Futino DO, Rocha-Junior CM, Amorim CA, Báo SN, Lucci CM. Cryopreservation of swine ovarian tissue: effect of different cryoprotectants on the structural preservation of preantral follicle oocytes. *Cryobiology* 2009;59: 195–200.
- [20] Shaw JM, Oranratnachai A, Trounson AO. Fundamental cryobiology of mammalian oocytes and ovarian tissue. *Theriogenology* 2000;53:59–72.
- [21] Lintern-Moore S, Moore GPM, Tyndale-Biscoe CH, Poole WE. The growth of the oocyte and follicle in the ovaries of monotremes and marsupials. *Anat Rec* 1976;185:325–32.
- [22] Lundy T, Smith P, O’Connell A, Hudson NL, McNatty KP. Population of granulosa cells in small follicles of the sheep ovary. *J. Reprod Fertil* 1999;115:251–62.
- [23] Domingues SFS, Furtado SHC, Ohashi OM, Rondina D, Silva LDM. Histological study of capuchin monkey (*Cebus apella*) ovarian follicles. *Acta Amazônica* 2004;34:495–501.
- [24] Morbeck DE, Esbenshade KL, Flowers WL, Britt JH. Kinetics of follicle growth in the prepubertal gilt. *Bio Fert Reprod* 1992;47:485–91.
- [25] Figueiredo JR, Hulshof SCJ, Van der Hurk R, Ectors JF, Bevers MM, Nusgens B, Beckers JF. Preservation of oocyte and granulosa cell morphology in bovine preantral follicles cultured in vitro. *Theriogenology* 1994;41:1333–46.
- [26] Makabe S, Van Blerkom J. Atlas of Human Female Reproductive Function: Ovarian Development to Early Embryogenesis After In-Vitro Fertilization, First Edition. Informa Healthcare, 2006.
- [27] Oktay K, Nugent D, Newton H, Salha O, Chatterjee P, Gosden RG. Isolation and characterization of primordial follicles from fresh and cryopreserved human ovarian tissue. *Fertil Steril* 1997;67:481–6.

- [28] Lucci CM, Kacinskis MA, Lopes LHR, Rumpf R, Báo SN. Effect of different cryoprotectants on the structural preservation of follicles in frozen zebu bovine (*Bos indicus*) ovarian tissue. *Theriogenology* 2004;61:1101–14.
- [29] Reader KL. A quantitative ultrastructural study of oocytes during the early stages of ovarian follicular development in Boorola and Wild-Type sheep. Victoria University of Wellington, Wallaceville, New Zealand, Thesis, 2007.
- [30] Fawcett DW. *An Atlas of Fine Structure—The Cell: Its Organelles and Inclusions*, W.B. Saunders Company, 1966.
- [31] Gunter KK, Gunter TE. Transport of calcium by mitochondria. *J Bioenerg Biomembr* 2004;26:471–85.
- [32] Maxfield FR, Wüstner D. Intracellular cholesterol transport. *J Clin Invest* 2002;110:891–8.
- [33] Dunbar BS, Avery S, Lee V, Prasad S, Schwahn D, Schwoebel E, Skinner S, Wilkins B. The mammalian zona pellucida: its biochemistry, immunochemistry, molecular biology and developmental expression. *Reprod Fertil Dev* 1994;6:331–47.
- [34] Bernhard W, Rouiller C. Close topographical relationship between mitochondria and ergastoplasm of liver cells in a definitive phase of cellular activity. *J Biophysic Biochem Cytol* 1956;2:73–8.
- [35] Russe I. Oogenesis in cattle and sheep. *Bibl Anat* 1983;24:77–92.
- [36] Adams EC, Hertig AT. Studies on guinea pig oocytes. Electron microscope observations on the development of cytoplasmic organelles in oocyte of primordial and primary follicles. *J Cell Biol* 1964;21:397–427.
- [37] Zamboni L. Fine morphology of the follicle wall and follicle cell–oocyte association. *Biol Reprod* 1974;10:125–49.
- [38] Nicosia SV, Evangelista I, Batta SK. Rabbit ovarian follicles. I. Isolation technique and characterization at different stages of development. *Biol Reprod* 1975;13:423–47.
- [39] Hilmelstein-Braw R, Byskov AG, Peters H, Faber M. Follicular atresia in the infant human ovary. *J Reprod Fertil* 1976;46:55–9.
- [40] Oakberg EF. Follicular growth and atresia in the mouse. *In vitro* 1979;15:41–9.
- [41] Anderson E, Albertini DF. Gap junctions between the oocyte and companion follicle cells in the mammalian ovary. *J Cell Biol* 1976;71:680–6.
- [42] Herlands RL, Schultz RM. Regulation of mouse growth: probable nutritional role for intercellular communication between follicle cells and oocytes: in oocyte growth. *J Exper Zoo* 1984; 229:317–25.
- [43] Basso AC, Esper CR. Isolation and ultrastructural characterization of preantral follicles in the Nelore breed cows (*Bos Taurus indicus*) *Braz J Vet Res Anim Sci* 2002;39:311–9.
- [44] Andrade ER, Maddox-Hyttel P, Landim-Alvarenga FDC, Silva JRV, Alfieri AA, Seneda MM, Figueiredo JR, Toniolli R. Ultrastructure of sheep primordial follicles cultured in the presence of indol acetic acid, EGF, and FSH. *Vet Med Int* doi: 10.4061/2011/670987.
- [45] Hayat MA. *Stains and Cytochemical Methods*, Plenun Publishing Corporation, 1993.
- [46] Didion BA, Pomp D, Martin MJ, Homancis GE, Markert CL. Observations on the cooling and cryopreservation of pig oocytes at the germinal vesicle stage. *J Anim Sci* 1990;68:2803–10.

[47] Nagashima H, Kashiwazaki N, Ashman RJ, Grupen CG, Seamark RF, Nottle MB. Removal of cytoplasmic lipid enhances the tolerance of porcine embryos to chilling. *Biol Reprod* 1994; 51:618–22.

[48] Isachenko V, Isachenko E, Michelmann JL, Alabart I, Vazquez N, Bezugly N, Nawroth F. Lipolysis and ultrastructural changes of intracellular lipid vesicles after cooling of bovine and porcine GV-oocytes. *Anat Histol Embryol* 2001;30:333–8.